Contents lists available at ScienceDirect

Earth and Planetary Science Letters

www.elsevier.com/locate/epsl

Calcification and growth processes in planktonic foraminifera complicate the use of B/Ca and U/Ca as carbonate chemistry proxies

Kate H. Salmon [a,*], Pallavi Anand [a], Philip F. Sexton [a], Maureen Conte [b,c]

[a] Department of Environment, Earth and Ecosystems, The Open University, Walton Hall, Milton Keynes, Buckinghamshire, MK7 6AA, UK
[b] Bermuda Institute of Ocean Sciences, St Georges, Bermuda
[c] Ecosystems Center, Marine Biological Laboratory, Woods Hole, MA 02543, USA
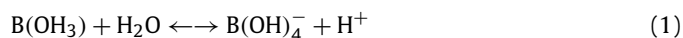
A B S T R A C T

Although boron and uranium to calcium ratios (B/Ca, U/Ca) in planktonic foraminifera have recently received much attention as potential proxies for ocean carbonate chemistry, the extent of a carbonate chemistry control on these ratios remains contentious. Here, we use bi-weekly sediment trap samples collected from the subtropical North Atlantic in combination with measured oceanographic data from the same location to evaluate the dominant oceanographic controls on B/Ca and U/Ca in three depth-stratified species of planktonic foraminifera. We also test the control of biological, growth-related, processes on planktonic foraminiferal B and U incorporation by using foraminifer test area density ($\mu g/\mu m^2$) (a monitor of test thickness) and test size from the same samples. B/Ca and U/Ca show little or no significant correlation with carbonate system parameters both within this study and in comparison with other published works. We provide the first evidence for a strong positive relationship between area density (test thickness) and B/Ca, and reveal that this is consistent in all species studied, suggesting a likely role for calcification in controlling boron partitioning into foraminiferal calcite. This finding is consistent with previous observations of less efficient discrimination against trace element 'impurities' (such as B), at higher calcification rates. We observe little or no dependency of B/Ca on test size. In marked contrast, we find that U/Ca displays a strong species-specific dependency on test size in all species, but no relationship with test thickness, implicating some other biological control (possibly related to growth), rather than a calcification control, on U incorporation into foraminiferal calcite. Our results caution against the use of B/Ca and U/Ca in planktonic foraminifera as reliable proxies for the ocean carbonate system and recommend that future work should concentrate on improving the mechanistic understanding of how planktonic foraminifer calcification and growth rates regulate boron and uranium incorporation into the test.
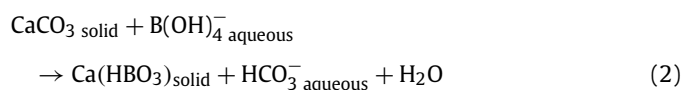
1. Introduction

B/Ca and U/Ca of planktonic foraminiferal calcite have previously been suggested to reflect the carbonate chemistry of seawater (Russell et al., 2004; Allen et al., 2011, 2012) and could potentially be used to reconstruct past ocean carbonate chemistry changes (Yu et al., 2007; Foster, 2008). Documenting past seawater carbonate chemistry changes is important in defining the processes that drive Earth's climate system and carbon cycle, and how these will respond to future anthropogenic climate change. Theoretically, boron exists in seawater as two species, boric acid [$B(OH_3)$] and

borate ion [$B(OH)_4^-$], the proportions of which are pH dependent, (see equilibrium equation (1) below).

$$B(OH_3) + H_2O \longleftrightarrow B(OH)_4^- + H^+ \qquad (1)$$

Because $B(OH)_4^-$ is a charged ion, it is thought that this is the only species which substitutes for CO_3^{2-} in calcite (Hemming and Hanson, 1992; Sanyal et al., 2000), and this has been supported by recent studies (Rae et al., 2011; Branson et al., 2015). Increasing pH therefore leads to greater incorporation of B in the $CaCO_3$ lattice due to increasing abundance of aqueous borate, (see equilibrium equation (2) below).

$$CaCO_{3\,solid} + B(OH)_{4\,aqueous}^-$$
$$\rightarrow Ca(HBO_3)_{solid} + HCO_{3\,aqueous}^- + H_2O \qquad (2)$$

* Corresponding author.
  E-mail address: k.h.salmon@gmail.com (K.H. Salmon).

This leads to an exchange distribution coefficient (K_D) (Yu et al., 2007), (see equilibrium equation (3) below).

$$K_D = [B/Ca]_{solid} / \left[B(OH)_4^- / HCO_3^- \right]_{seawater} \qquad (3)$$

However, a variety of evidence also exists arguing against a primary carbonate control on B/Ca ratios including: (1) The lack of correlation of B/Ca and pH-dependent boron isotope composition (Foster, 2008) and measured carbonate system parameters (Babila et al., 2014), (2) Higher B/Ca in upwelling regions despite lower pH conditions (Naik and Naidu, 2014), (3) Species-specific sensitivities of B/Ca to carbonate chemistry (Allen and Hönisch, 2012), (4) Size-dependent B incorporation into foraminiferal calcite (Yu et al., 2007; Babila et al., 2014; Henehan et al., 2015), (5) Discrepancies between culture and open-ocean studies of the sensitivity of B/Ca to $[CO_3^{2-}]$ (Yu et al., 2007; Allen and Hönisch, 2012). Additionally, a number of other environmental variables have been reported to influence B concentrations in foraminiferal calcite including, temperature (Hathorne et al., 2009; Naik and Naidu, 2014), salinity (Allen et al., 2011, 2012; Henehan et al., 2015), light intensity (Babila et al., 2014), and $[PO_4^{3-}]$ (Henehan et al., 2015).

As with boron, uranium incorporation into planktonic foraminifera is also theoretically controlled by $[CO_3^{2-}]$ because it exists in seawater as a series of carbonate complexes and is likely incorporated into calcite as either $UO_2(CO_3)_2^{2-}$ and/or $UO_2(CO_3)_3^{4-}$ (Yu et al., 2008 and references therein). Therefore, the decreasing abundance of $UO_2(CO_3)_2^{2-}$ with greater $[CO_3^{2-}]$ should also be reflected by decreasing foraminiferal U/Ca (Russell et al., 2004). Yet, like boron, a number of other variables in addition to the carbonate system have been suggested to also influence U incorporation, including calcification temperature (Russell et al., 1996; Yu et al., 2008), growth rate (Ni et al., 2007), and species-specific differences (Yu et al., 2008).

Here, we utilise bi-weekly samples from a sediment trap time series from the subtropical North Atlantic (Salmon et al., 2015) to address the unresolved and potentially conflicting issues with these proxies. Sediment trap time series provide a unique opportunity to evaluate controls on the geochemical composition of planktonic foraminifera within their natural habitat where multiple variables influence their calcification simultaneously. This contrasts with laboratory methods, which although have been instrumental in ground-truthing relationships between geochemical proxies and environmental variables, typically isolate only single variables to determine their influence on foraminiferal calcite. The bi-weekly sampling resolution provided by the sediment traps is also advantageous because it captures the lifecycles of most planktonic foraminiferal species, which typically follow the monthly lunar cycle (Jonkers and Kučera, 2015), with evidence of an annual cycle for encrusted *Globorotalia truncatulinoides* (Hemleben et al., 1985; McKenna and Prell, 2004). We measured B/Ca and U/Ca ratios, test calcification (thickness) and growth parameters (size) of three planktonic foraminifer species from bi-weekly sediment trap samples spanning four years (1998–2000 and 2008–2010), from the Sargasso Sea (Fig. 1a). These data were coupled with in-situ oceanographic data (temperature, salinity, chlorophyll and carbonate system parameters) from the Bermuda Atlantic Time Series (BATS) in the same locality to evaluate the controls on uranium and boron incorporation into planktonic foraminifera (Fig. 1b–c).

2. Materials and methods

We use bi-weekly sediment trap samples selected from the Ocean Flux Programme time series in the Sargasso Sea (31°50′N, 64°10′W) together with the concurrent oceanographic data from the nearby BATS site (31°40′N, 64°10′W). We utilise samples collected from two equivalent 2.5-yr intervals (1998–2000 and 2008–2010) at 1500 m water depth to capture seasonal variations in the test parameters and geochemical composition of three species of foraminifera (*Globigerinoides ruber* (pink), *Orbulina universa* and *Globorotalia truncatulinoides*, non-encrusted (nc) and encrusted (c)), each living at different depths in the water column. Test weights and sizes were measured individually in order to calculate test area density ($\mu g/\mu m^2$) of each sample (details in section 2.3).

Tests used for geochemical analysis ranged in size (shown in Table 2), but on average were *G. ruber* (p) = 366 µm, *O. universa* = 720 µm, *G. truncatulinoides* (nc) = 492 µm, *G. truncatulinoides* (c) = 709 µm. *G. truncatulinoides* reproduce in the surface waters, as evidenced from plankton tows (Hemleben et al., 1985) before sinking to depth and adding a secondary calcite crust which approximately doubles the weight of the test (McKenna and Prell, 2004). Figure A.1 provides guidance for conversion of digitally measured test size to traditional sieve sizes. We used the right-coiling variety of *G. truncatulinoides* in this study which all belong to the same genetic group (Type II) (Ujiié et al., 2010), as this is the dominant genotype present at our Sargasso Sea study site. Likewise, we analyse the more abundant thinner shelled Sargasso genotype of *O. universa*, which is morphologically distinct under high magnification, from the thicker-walled Caribbean genotype (Morard et al., 2009). By selecting species from a wide range of water depth habitats (approximately 0–400 m), we are able to compare oceanographic data with species' geochemical compositions across larger environmental gradients; e.g. from 0–400 m at this site, temperature ranges up to ∼10 °C (Fig. 1b) and $[CO_3^{2-}]$ by ∼50–60 µmol/kg (Fig. 1c), with a minimal change in salinity (∼0.2).

After being measured, planktonic foraminifera tests were gently cracked to open and subjected to chemical cleaning involving an extended oxidation step to remove any excess organic matter present in sediment trap material (50% H_2O_2 in 0.2M NaOH) (Anand et al., 2003), followed by a weak acid leach, prior to final dissolution (Barker et al., 2003). B/Ca and U/Ca analyses were carried out on a Thermo® Element XR Inductively-Coupled Plasma Mass Spectrometer (HR-ICP-MS), at the Godwin Laboratory at Cambridge University. Long-term precision on standard runs of B/Ca (and Mg/Ca used for calcification temperatures calculations) is <1.0% (2σ). External precision is <4.0% (2σ) for B/Ca and U/Ca, and <1.0% (2σ) for Mg/Ca using Cambridge consistency standards (Misra et al., 2014). B, Mg blank levels were <2% and U was <5% of typical [B], [Mg] and [U] in foraminifera samples. An in-house standard was used to correct for drift over the run.

2.1. Calcification temperature and depth calculations

Calcification temperatures were determined from analysing the $\delta^{18}O_{calcite}$ in the same aliquot of sample used for trace element analyses. Stable isotope analyses were performed on a Finnigan GasBench and Delta^{plus} Advantage stable isotope mass spectrometer at the Open University (long term standard reproducibility is ±0.084‰ for $\delta^{18}O$ and ±0.061‰ for $\delta^{13}C$) and are reported relative to Vienna Pee Dee Belemnite (V-PDB). Temperature and salinity data from different depth habitats were taken from the Bermuda Atlantic Time Series (BATS) to calculate the $\delta^{18}O$ of calcite in equilibrium with seawater ($\delta^{18}O_{sw}$). The $\delta^{18}O_{sw}$ at Bermuda was calculated using the 0–50 m $\delta^{18}O_{sw}$-salinity relationship for the tropical–subtropical Atlantic available through the NASA seawater database (Arbuszewski et al., 2010; Schmidt et al., 1999). Calcification temperatures were then calculated using $\delta^{18}O_{calcite}$ and calculated $\delta^{18}O_{sw}$ where available. For *G. ruber* (p) and *G. truncatulinoides*, we use the rearrangement of the palaeotemperature equation of O'Neil et al. (1969) and Shackleton (1974) and for *O. universa*, we used the low-light palaeotemperature equation of Bemis et al. (1998). For samples where no stable isotope data
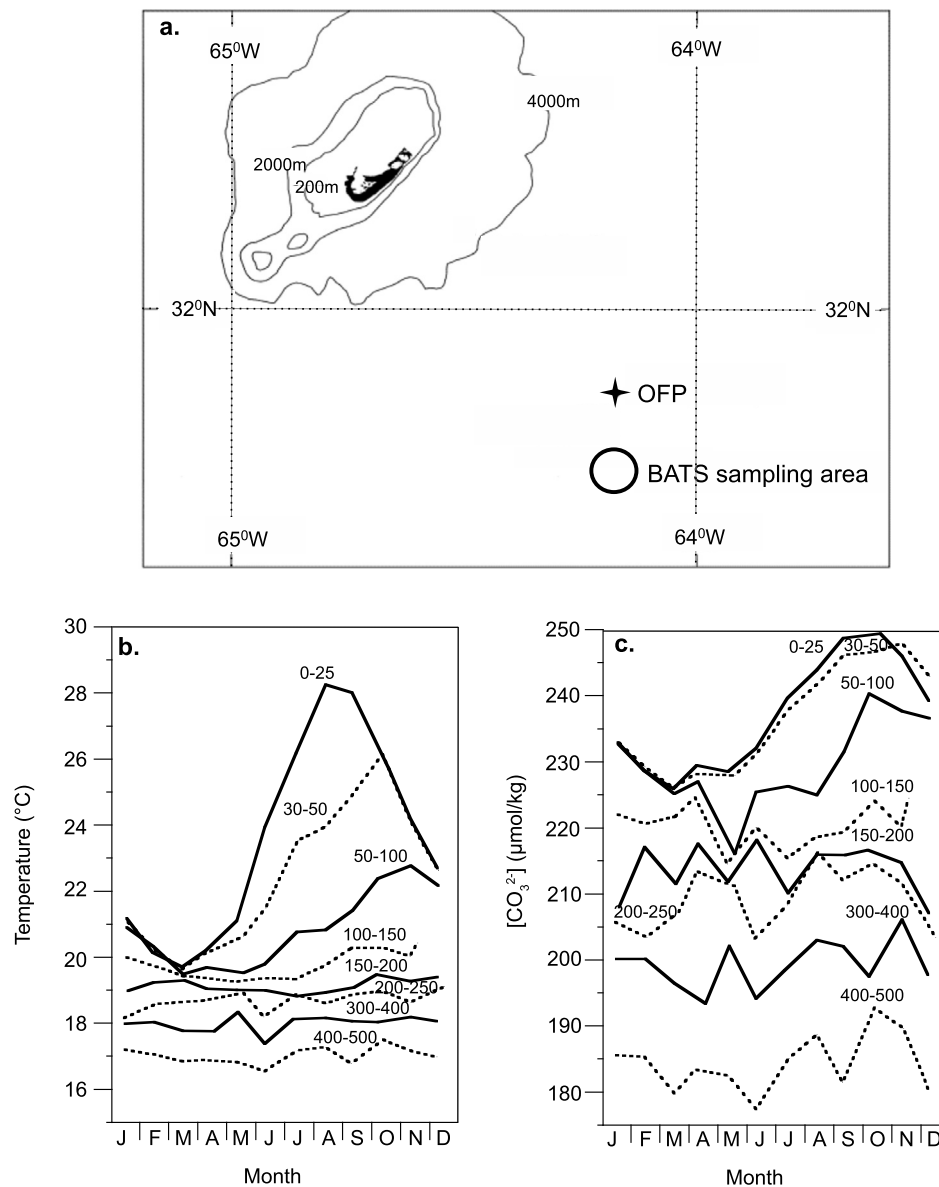
Fig. 1. a. Map to show the location of the Oceanic Flux Program (OFP) sediment traps and the Bermuda Atlantic Time Series (BATS) oceanographic data station in relation to Bermuda Island. **b**. Annual cycles of temperature, **c**. [CO_3^{2-}] from BATS hydrographic station, averaged over the same time period as the sediment trap deployments (1998–2000 and 2008–2010). Numbers on the plots are water depths in metres.

were available, we use species-specific Mg/Ca-temperature calibration equations to calculate the calcification temperatures and associated depth habitats (Anand et al., 2003). In order to estimate depth habitats, we then matched these calcification temperatures for individual samples to BATS oceanographic temperatures measured in the previous month to account for foraminifer lifecycle and settling time (see section 2.2 for more details). The depth at which the oceanographic temperature most closely matches the calcification temperature is then used to denote the approximate depth habitat, similar to previous a study (Marshall et al., 2013).

Spero et al. (1997) previously observed a [CO_3^{2-}] influence on $\delta^{18}O_c$ of *O. universa* in culture. In order to test for this, we used the $\Delta\delta^{18}O$–[CO_3^{2-}] model developed by King and Howard (2005) where $\Delta\delta^{18}O$ represents the difference between measured $\delta^{18}O_{calcite}$, and predicted $\delta^{18}O_{calcite}$ calculated from instrumental temperatures collected at BATS. We find no correlation between $\Delta\delta^{18}O$ and [CO_3^{2-}] (Figure A.2), so no correction was applied here.

2.2. Carbonate parameter calculations

In-situ seawater carbonate system parameters were calculated using monthly oceanographic data obtained from the BATS database (http://bats.bios.edu/bats_methods.html). Assuming an average 3–4 week lifespan of *G. ruber* (p) and *O. universa* (Jonkers and Kučera, 2015) and a 5-day settling period to reach the 1500 m trap (~300 m/day, Takahashi and Bé, 1984; Marshall et al., 2013), we selected oceanographic data approximately 1 month before the mid-date of the sediment trap opening period to account for the typical lifespan of a foraminifer. Encrusted *G. truncatulinoides* likely reproduces on an annual cycle (McKenna and Prell, 2004) but numerous non-encrusted specimens are found in the surface waters during the winter months after adult specimens reproduce (Hemleben et al., 1985; Spear et al., 2011), so we also used oceanographic data from ~1 month before the trap opening for non-encrusted *G. truncatulinoides*. We then selected an oceanographic temperature that best matched the calcification temperature for that species in that sample. All of the oceanographic data asso-

ciated with this temperature (including all of the carbonate data, salinity, and productivity parameters) were then used in accordance with these shell measurement and geochemical data. The temperature, salinity, and two carbonate parameters (dissolved inorganic carbon, total alkalinity data) were then inputted into the CO2Sys_v2.1.xls program (Pelletier et al., 2007) in order to calculate the remaining carbonate system parameters. We applied the carbonic acid dissociation constant of Mehrbach et al. (1973), refit by Dickson and Millero (1987) and the dissociation constant for HSO_4^- (Dickson, 1990).

2.3. Calcification and test size data

Previous studies have shown that size-normalised weights (SNWs) or area density (a proxy for shell thickness) of planktonic foraminifera may reflect variations in foraminiferal calcification, mainly related to changes in seawater $[CO_3^{2-}]$ (Barker and Elderfield, 2002; Marshall et al., 2013 and references therein). SNWs are calculated by weighing batches of shells in narrow sieve-size 'windows' (Beer et al., 2010), but this method has largely been superseded by a more precise measurement termed area density ($\mu g/\mu m^2$). Area density measurements are calculated using individual, digitally measured test areas normalised to individual test weights ($\mu g/\mu m^2$). We use the average area density of a number of individually measured tests ($n = 6$–30) to represent the area density for each sample (Table B.2). This technique allows for a more accurate estimation of relative changes in shell wall thickness (Marshall et al., 2013).

Although changes in planktonic foraminiferal shell thicknesses represent a complex physiological process and are not directly comparable to the controls on inorganic calcite precipitation rates, previous observations of a positive relationship between SNW or area density and $[CO_3^{2-}]$ (Marshall et al., 2013 and references therein), are consistent with observations of increasing calcite precipitation 'rates' in higher pH seawater (Ruiz-Agudo et al., 2012). However, since foraminifera calcify intermittently during their growth, their calcification rates will inherently vary throughout their lifecycles. Because the lifecycles of both *G. ruber* (p) and *O. universa* are externally controlled by the lunar cycle (Jonkers and Kučera, 2015), both species likely calcified over comparable time periods (3–4 weeks). Likewise, non-encrusted *G. truncatulinoides* do not incorporate any secondary calcite so most likely calcified in the surface waters for a few weeks before the sinking to the trap (Spear et al., 2011). Therefore, the area densities of all three species used in this study (excluding encrusted *G. truncatulinoides*) represent the intermittent precipitation of calcite over comparable intervals of time. In the context of this study, we use foraminifera test area density to document the average of these intermittent calcification rates over the lifespan of a foraminifer, where greater area densities represent thicker gross test walls and thus faster calcification rates averaged across these intermittent windows of calcification. Area densities thus reflect biologically mediated calcification and are not directly synonymous with inorganic calcite precipitation rates.

Individual foraminifera tests were weighed on a XS Mettler Toledo microbalance and photographed in the same orientation, under a stereomicroscope for size analysis. We calibrated ImageJ analysis software using a microscale image taken at the same magnification as foraminifera tests and adjusted the image threshold to determine 2D silhouette areas of individual tests. Errors on area density measurements were defined as AD $\pm(1/n)$ (Marshall et al., 2013). Individual test size data of shells within each sample were used to evaluate biological control of B and U incorporation in planktonic foraminifera (Salmon K., unpublished PhD Thesis, 2015). In line with previous work, we interpret higher area densities as

representing thicker shells and hence a greater gross rate of calcification over the lifetime of the foraminifer (Marshall et al., 2013).

2.4. Multiple linear regression

We performed multiple linear regression analyses using the function 'lm' in R (http://www.r-project.org) to test which of the independent environmental (e.g. carbonate chemistry, temperature, salinity, chlorophyll) and ecological parameters (e.g. test size/area density) explain the variance in the dependent variables i.e. B/Ca and U/Ca. The selections of these independent variables are based on previous observations of temperature (Yu et al., 2008), salinity (Allen et al., 2011; Henehan et al., 2015), carbonate chemistry (Yu et al., 2007, 2013; Allen et al., 2011, 2012), secondary crust formation (Hathorne et al., 2009) and size fractionation (Elderfield et al., 2002; Ni et al., 2007; Friedrich et al., 2012) related to calcification/growth rate (we use area density/test size as a proxy) (Ni et al., 2007; Naik and Naidu, 2014) affecting the incorporation of B and U into the foraminiferal test. We use chlorophyll concentration to test how changes in productivity could affect trace element ratios in samples where these data are available (Table B.2). It is important to note that area densities and test sizes of *G. truncatulinoides* are positively correlated because tests grow simultaneously larger and thicker, so these shell parameters cannot be decoupled in this species. Our subtropical gyre has negligible dissolved phosphate present in surface waters (Steinberg et al., 2001) meaning we were unable to explicitly test a recently observed B/Ca relationship with $[PO_4^{3-}]$ in planktonic foraminifera (Henehan et al., 2015). For each analysis, non-contributing factors were removed according to their contribution to Akaike Information Criterion (AIC) (Akaike, 1974). AIC provides a statistical framework in which to select a model with the least number of parameters required in order to achieve the best fit. Lower values of the index indicate the model with the fewest parameters that still provides an adequate fit to the data.

The more sensitive the dependent variable is to changes in the independent variable, the greater the value of the slope coefficient in the regression. We have repeated the analyses using a multispecies model, and species-specific models for *O. universa* and *G. truncatulinoides* (non-encrusted and encrusted). We were too limited by sample sizes to produce reliable species-specific models for *G. ruber* (p) and non-encrusted *G. truncatulinoides*. We have intentionally excluded encrusted *G. truncatulinoides* from the multispecies model because the presence of secondary crust in this species may bias our results. Confidence in the species-specific *O. universa* model is reduced compared to the other models owing to the small sample size relative to the number of independent variables.

3. Results

3.1. Seasonality in B/Ca, U/Ca and calcification temperatures

The seasonal range in calcification temperatures (calculated from a combination of $\delta^{18}O$ and Mg/Ca), varies from 15–30 °C for all three species over both the sediment trap deployment periods. This is on average within the range of estimated calcification depths for each species ~16 m for *G. ruber* (p) and ~68 m for *O. universa* (Fig. 2a) (see Table B.2). Generally, most of the non-encrusted *G. truncatulinoides* appear to calcify in the surface waters during winter corresponding to an average calcification depth of ~44 m, but a cold-core cyclonic eddy in February–March 2010 caused anomalously low surface water temperatures as indicated by low calcification temperatures in Fig. 2a. Encrusted *G. truncatulinoides* predominantly reside at depths of ~300–400 m throughout
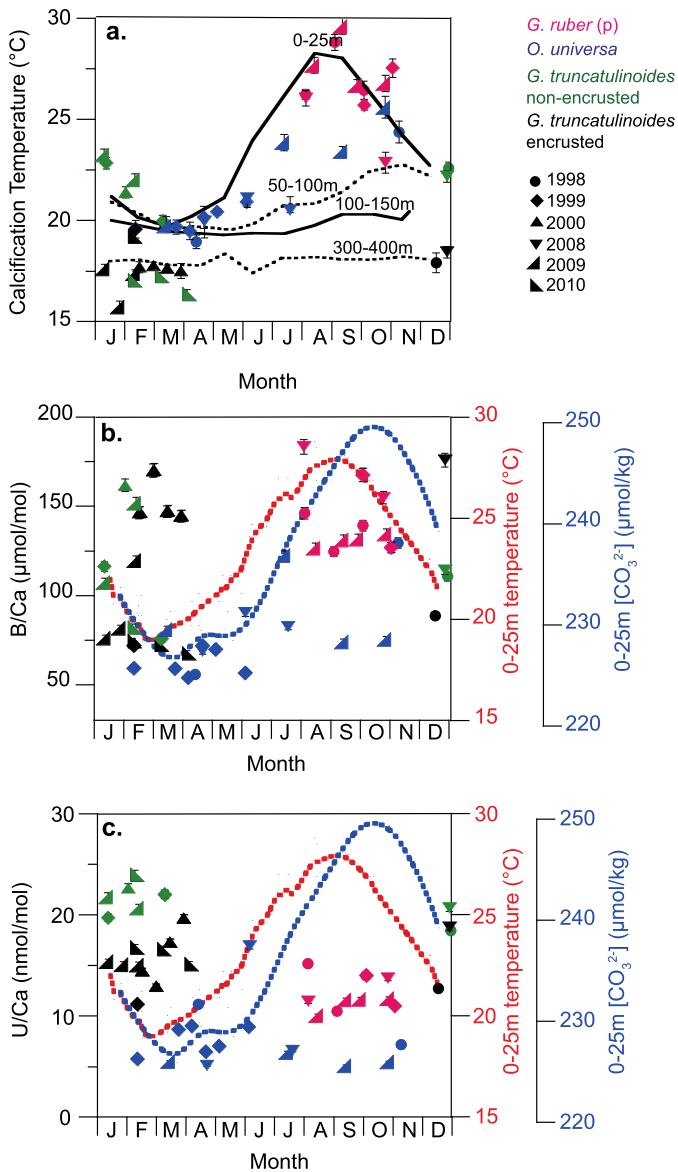
Fig. 2. a) Seasonal changes in calcification temperatures (inferred from $\delta^{18}O$ isotopes and Mg/Ca) of *G. ruber* (p) (pink), *O. universa* (blue), *G. truncatulinoides* encrusted (black) and non-encrusted (green) with interannual variability represented as different symbols. **b)** seasonal B/Ca and **c)** seasonal U/Ca. Depth horizons as well as seasonal changes in 0–25 m temperature (red, dotted lines) and $[CO_3^{2-}]$ (blue, dotted lines) are added for reference and represent average monthly data combined for years 1998–2000 and 2008–2010 to give an approximate visualisation of depth habitat. Please see Table B.2 for more accurate depth estimates. The errors on calcification temperatures are detailed in Table B.2. The errors on internal standard measurements (σ) are B/Ca = ±1.84%, U/Ca = ±1.79%, in Cambridge consistency standards containing <20, ~85 and ~200 µmol/mol B/Ca and ~45–65 nmol/mol U/Ca stated in Misra et al. (2014).

the winter, and some non-encrusted individuals calcify at 0 m (Fig. 2a).

Generally, the higher B/Ca of *G. ruber* (pink) coincides with warmer summer temperatures and greater $[CO_3^{2-}]$ compared to *O. universa*. However, within species, the B/Ca of *G. ruber* (p) and *O. universa* do not appear to change with temperature or $[CO_3^{2-}]$ (Fig. 2b). The range of B/Ca in *G. truncatulinoides* alone is equal to the combined range of *G. ruber* (p) and *O. universa* (~110 µmol/mol), despite this species living in a more limited range of winter temperatures and $[CO_3^{2-}]$ (Fig. 1b–c). Non-encrusted *G. truncatulinoides* contain greater U/Ca than encrusted individuals but this is not so for B/Ca. Like B/Ca, the U/Ca of *G. ruber* (p) is greater than U/Ca in *O. universa* and ranges from

~5 nmol/mol in *O. universa* to 15 nmol/mol in *G. ruber* (p). *G. truncatulinoides* has the largest range in U/Ca (~13 nmol/mol) and is also positively offset from *G. ruber* (p) and *O. universa* (Fig. 2c).

3.2. Controls on trace element incorporation

Table 1 displays the multiple linear regression (MLR) results. Contrary to previous observations in culture, we see no significant $[CO_3^{2-}]$ effect on B/Ca and only a small proportion of the variance in U/Ca of *G. ruber* (p), *O. universa* and non-encrusted *G. truncatulinoides* is explained by both area density and $[CO_3^{2-}]$ ($r^2 = 0.24$). Replacing $[CO_3^{2-}]$ with other carbonate system drivers such as $[B(OH)_4^- / HCO_3^-]_{seawater}$ or pH in the model also yields no significant relationship with B/Ca. Instead, area density/test thickness appears to explain the majority of the variance in B/Ca of *G. ruber* (p), *O. universa*, and non-encrusted *G. truncatulinoides* (Table 1). Although calcification temperature appears to explain some variance in B/Ca of all species, this could be an artefact of combining species over a large depth range, because it is not significant in explaining species-specific B/Ca variations in *O. universa* or *G. truncatulinoides* individually (Table 1). The small range in salinity at this site does not appear to control any variance in B/Ca or U/Ca. Likewise, chlorophyll concentrations, used as an indicator of productivity, do not exert any significant control over B/Ca or U/Ca in any of the species tested (although chlorophyll could not be tested in encrusted *G. truncatulinoides*, below the euphotic zone). None of our tested parameters exert any significant control on B/Ca in encrusted and non-encrusted *G. truncatulinoides* only, but area density/test thickness and test size explain most of the variation in U/Ca in this species ($r^2 = 0.90$) (Table 1).

We aimed to keep our measurements within as narrow test size ranges as possible but *G. truncatulinoides* has a larger variance in size due to growth and addition of crust (Table 2). We find a correlation between test size and intra-species variations in U/Ca and B/Ca in most species (Table 2). Higher B/Ca values significantly correlate with larger tests but only in *G. ruber* (p) and the relationship is weak ($r^2 = 0.43$) compared to higher U/Ca strongly associated with larger tests in all species ($r^2 = 0.52$–0.81), except encrusted *G. truncatulinoides* (Table 2).

4. Discussion

4.1. Oceanographic controls on foraminifera B/Ca and U/Ca

4.1.1. Carbonate chemistry

U/Ca and B/Ca have been previously suggested as proxies for the ocean carbonate system based on laboratory culturing experiments (Sanyal et al., 1997; Allen et al., 2011, 2012). However, our field study in context with others shows that overall, regardless of which carbonate parameter is used to represent carbonate chemistry, there is no significant influence on B incorporation (Fig. 3a). Likewise, along with area density, carbonate chemistry only explains 24% of the variations in the U/Ca of *G. ruber* (p), *O. universa*, and non-encrusted *G. truncatulinoides* (Table 1). Hypothetically, the seasonal range of 30 µmol/kg $[CO_3^{2-}]$ in *O. universa* at this site should be equivalent to a 0.7 nmol/mol change in U/Ca, according to laboratory culturing work on the same species (Russell et al., 2004). Yet this predicted 0.7 nmol/mol range in *O. universa* U/Ca is much smaller than the ~6 nmol/mol change we actually observe (Fig. 2c). Instead, much of the U/Ca variability can be explained through test size fractionation in individual species (Table 1–2).

The 60–75 µmol/mol range in B/Ca in *G. ruber* (p) and *O. universa* observed in this study only corresponds to a range in $[CO_3^{2-}]$ of 18–30 µmol/kg in respectively (Fig. 2b). However, according to laboratory culturing calibrations on the same species, this 60–75 µmol/mol range in B/Ca should equate to a range in $[CO_3^{2-}]$

Table 1
Shows the multiple linear regressions for all species (excluding encrusted *G. truncatulinoides*), *O. universa* only, and both encrusted and non-encrusted *G. truncatulinoides*. *G. ruber* (p) was not tested individually due to the low sample number in relation to the number of variables tested. Coefficients indicate the slope value or 'sensitivity' of the relationship between the variable and trace element ratio. Substituting in $[B(OH)_4^-/HCO_3^-]$ or pH in for $[CO_3^{2-}]$ makes no difference to the outcome of the multi-species B/Ca regression. Test size was not applied in the multi-species regression because it is species-specific. Samples with missing data for specific variables were not included in any regressions. Coefficients shown in bold refer to variables that were included in a second regression after selection according to the lowest AIC values (see section 2.4 for more details). The r^2 values reflect the outcome of the modelled variables highlighted in bold. Adjusted r^2 accounts for sample size and number of independent variables. Variables which contribute significantly to the model are starred as follows: * $p < 0.05$, ** $p < 0.01$, *** $p < 0.001$.

Variable	All species		*O. universa* only		*G. truncatulinoides* only	
	B/Ca	U/Ca	B/Ca	U/Ca	B/Ca	U/Ca
Area density	**90.95*****	**8.900***	**99.93****	3.100	−1.407	**−7.377*****
Test size	–	–	−0.054	**0.066*****	0.031	**0.0016****
Calcification temperature	**3.619***	−0.745	**3.324**	−0.155	0.854	0.035
$[CO_3^{2-}]$	0.596	**0.283***	−0.152	−0.0235	−0.339	0.0059
Salinity	15.55	2.787	24.11	4.573	**144.68**	0.671
Chlorophyll	−0.029	0.0047	**−0.056**	−0.0074	–	–
Multiple r^2	0.76	0.32	0.75	0.58	0.31	0.92
Adjusted r^2	0.74	0.24	0.67	0.55	0.24	0.90

Table 2
Coefficients of determination (r^2) of trace element-test size regressions of selected planktonic foraminifera species. Size ranges indicate minimum to maximum sizes of tests used in geochemical analysis. Values in bold indicate significant correlations * $p < 0.05$, ** $p < 0.01$, *** $p < 0.001$.

Intra-species size effect				
Trace element	*G. ruber* (p) (size range = 311–431 μm)	*O. universa* (size range = 657–792 μm)	*G. truncatulinoides* (non-encrusted) (size range = 347–720 μm)	*G. truncatulinoides* (encrusted) (size range = 509–796 μm)
B/Ca	**0.44***	−0.18	0.32	0.23
U/Ca	**0.53****	**0.58*****	**0.81*****	0.28

that is over an order of magnitude greater (∼300–>600 μmol/kg) (Allen et al., 2011, 2012). Indeed, the full range of all species' B/Ca recorded in this study (∼110 μmol/mol) should be equivalent to a pH range of ∼0.6 according to culture calibration (Allen et al., 2012) but we only see a ∼0.1 unit change in pH over the depth habitats of all species. Comparison of our results with other core-top and sediment-trap based studies shows that our sediment-trap data yield the largest range in B/Ca with one of the smallest ranges in $[CO_3^{2-}]$ (Fig. 3a). The lack of a distinct relationship between B/Ca and $[CO_3^{2-}]$ in this study, and other studies and species clearly indicates the existence of additional competing controls on boron incorporation in the natural environment.

One primary control on B/Ca could be $[B(OH)_4^-/HCO_3^-]_{seawater}$ (equation (3)), which is a function of temperature and pH (Allen et al., 2012). However, we find no correlation between either $[B(OH)_4^-/HCO_3^-]_{seawater}$ or pH and foraminiferal B/Ca. As previously shown at this site in *G. ruber* (white), seasonal temperature and pH variance only cause negligible variations in $[B(OH)_4^-/HCO_3^-]_{sw}$ (Babila et al., 2014), equivalent to a 3–5 μmol/mol change in B/Ca according to the calibration from Allen et al. (2012), just a fraction of the total ∼110 μmol/mol B/Ca range observed here (Fig. 3b).

4.1.2. Calcification temperature

In general, there is too much scatter to conclude there is any significant relationship between temperature and B/Ca (Fig. 3c). The lack of intra-species correlations of B/Ca and temperature, suggests that significant correlations highlighted in Table 1 could be an artefact of comparing multiple species. Yu et al. (2008) suggested that uranium incorporation into planktonic foraminifer calcite was strongly influenced by calcification temperature, based on core-top sediments. However, our sediment trap data reveal no significant relationship between uranium and temperature in any of the species that we examined (Table 1).

4.2. Biological controls on B/Ca and U/Ca

4.2.1. Calcification rate and test size

We find that B/Ca displays a strong positive correlation with area density, pointing to a calcification control on boron incor-

poration in *G. ruber* (p), *O. universa* and non-encrusted *G. truncatulinoides* (Fig. 4a). Although area density reflects the complex physiological process of biological calcification, and is not a direct measure of the rate of inorganic calcite precipitation, the inter-species correlation between area density and B/Ca is consistent with recent inorganic precipitation experiments which observed a dependency of boron incorporation on calcite precipitation rate (Ruiz-Agudo et al., 2012; Gabitov et al., 2014). If we assume that higher area densities represent faster calcification rates, as suggested by previous investigations (Spero et al., 1997; Marshall et al., 2013 – references therein), our results suggest that calcite growth rates, even when biologically mediated, could affect boron partitioning. This mechanism may explain why thicker tests with higher area densities contain more boron.

G. ruber (p) is the only species where B/Ca has a (weak) correlation with test size ($r^2 = 0.43$) (Fig. 4b), whereas U/Ca has a strong positive correlation with test size in all species ($r^2 = 0.52$–0.81) (Table 2) (Fig. 4d). This is consistent with previous observations of greater B/Ca in larger tests of *G. ruber* (white and pink) (Ni et al., 2007; Babila et al., 2014; Naik and Naidu, 2014; Henehan et al., 2015) and U/Ca in larger *G. ruber* (white and pink) and *G. sacculifer* tests (Ni et al., 2007). Most studies have attributed this test size fractionation to faster foraminiferal growth (where growth is represented by increases in chamber formation, not crystallographic precipitation) and calcification rates in larger individuals (Ni et al., 2007; Babila et al., 2014; Naik and Naidu, 2014). A faster calcification rate may be less effective at discriminating against incorporation of trace elements causing the organism to incorporate higher concentrations into its calcite lattice (Rickaby et al., 2002; Russell et al., 2004; Ni et al., 2007; Schmidt et al., 2008). However, if this were the case in all of our species, we would also expect to see a stronger positive relationship between U/Ca and area density (Fig. 4c), and also a positive relationship between B/Ca and test size in *O. universa* and non-encrusted *G. truncatulinoides* (Fig. 4b), but we do not. Whilst assuming larger tests grow faster and hence have faster calcification rates appears to be a deduction inconsistent with the majority of our data, it may be true for at least some species, such as *G. ruber* (white and pink). For instance, Babila et al. (2014) ob-
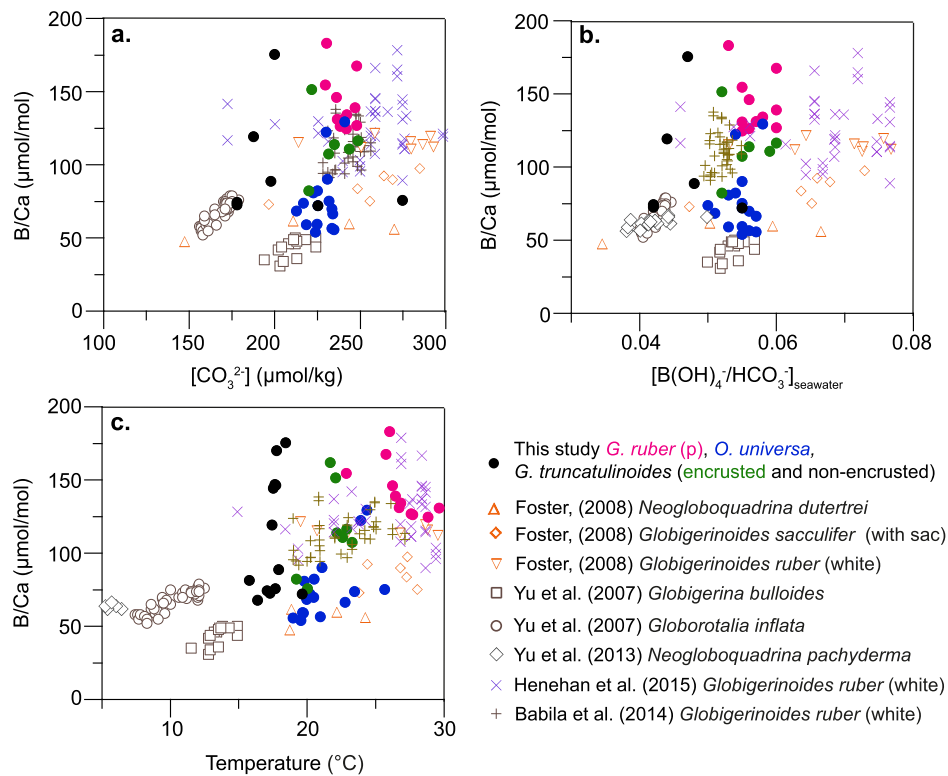
Fig. 3. Potential controls on boron incorporation: B/Ca from this study and other planktonic species varying with **a)** $[CO_3^{2-}]$ and **b)** $[B(OH)_4^-/HCO_3^-$ seawater] **c)** Temperature. Data from Babila et al. (2014) is an average of 20–40 m. Figures show open-ocean data only.

served a 15–20 μmol/kg offset in B/Ca between the 200–300 and 300–400 μm size fractions of *G. ruber* (white). Although they attribute this offset between size fractions to increased light intensity governing greater boron incorporation in larger tests due to a greater density of symbionts, we suggest that it could equally arise from increased growth/calcification rates in larger tests. We find that area densities in larger *G. ruber* (p) tests from this study are on average higher, when compared to area densities from smaller tests; 311–363 μm (equivalent sieve size = 250–300 μm, Figure A.1) = area density of 1.23×10^{-4} μg/μm, compared to 371–431 μm (equivalent sieve size = 300–355 μm, Figure A.1) = area density of 1.34×10^{-4} μg/μm. We find this offset in area densities between larger and smaller tests of *G. ruber* (p) is equivalent to a ∼22 μmol/kg offset in B/Ca, almost the same discrepancy observed between sieve-size fractions by Babila et al. (2014). Yet Babila et al. (2014) discounted a calcification rate control on B/Ca because they do not see a similar offset between size fractions for Sr/Ca and Mg/Ca. However, a calcification rate control would not necessarily have to be reflected in both Mg/Ca and Sr/Ca to be plausible in B/Ca. Ni et al. (2007) concluded there was no calcification control on Mg/Ca in *G. sacculifer* and *G. ruber* even though there was in B/Ca, Li/Ca and U/Ca. Additionally, we discount a light intensity control on B incorporation in this study based on three observations. First, we find no correlation between test size or B/Ca and $\delta^{13}C$ in symbiont-bearing *G. ruber* (p) or *O. universa* (which would be enhanced in larger tests with more symbiont activity due to greater carbon fixation, Spero and Parker, 1985) (see Figure A.3a–b). Second, we also see no effect of test size on boron incorporation in symbiont-bearing *O. universa* (Fig. 4b). Third, non-encrusted symbiont-barren *G. truncatulinoides* possess a greater B/Ca concentration than *O. universa*, and comparable B/Ca to *G. ruber* (p) (Fig. 4a), which should not be the case if its incorporation were primarily controlled by symbionts enhancing microenvironment pH (Figure A.3a–b).

Recently, an observed correlation between $[PO_4^{3-}]$ and B/Ca ratios in *Globigerinoides ruber* led to the suggestion that $[PO_4^{3-}]$ may be a control on foraminiferal B/Ca (Henehan et al., 2015). These authors proposed that this may arise from chemical interactions involving P at the mineral–water interface, either through paired substitution, increased disorder in the crystal lattice, or perhaps by stabilisation of an amorphous calcium carbonate precursor phase. However, $[PO_4^{3-}]$ at our subtropical gyre site is negligible in the surface waters and only reaches 0.26 μmol/kg at ∼400 m (Steinberg et al., 2001), which according to the approximate B/Ca–$[PO_4^{3-}]$ relationship described by Henehan et al. (2015), should be equivalent to ∼30 μmol/mol change in B/Ca, just a quarter of our observed 110 μmol/mol range. In addition, we observe higher foraminiferal B/Ca at our site (*G. ruber* (p) and non-encrusted *G. truncatulinoides*) than Henehan et al. (2015) does in *G. ruber* (w), even in our relatively $[PO_4^{3-}]$-depleted surface waters, which further argues against a dominant $[PO_4^{3-}]$ control. Although our data do not allow us to explicitly test the hypothesis of crystallographic interaction between foraminiferal B/Ca and $[PO_4^{3-}]$ (Henehan et al., 2015), we suggest that the positive correlation between B/Ca in *G. ruber* (w) and $[PO_4^{3-}]$ could be caused by higher growth and calcification rates, which coincide with areas of higher productivity. This is consistent with other studies that have observed greater B/Ca in larger (and hence faster growing) *G. ruber* (w) tests during upwelling periods (Naik and Naidu, 2014) and also in cultured foraminifera fed every day, compared to lower B/Ca in open-ocean foraminifera from a comparable pH (Henehan et al., 2015). We do not observe a significant relationship between chlorophyll and foraminifera B/Ca variations, suggesting that productivity is not the dominant control on foraminiferal calcification and hence boron incorporation at this site.

In contrast to B/Ca, we observe greater U/Ca in non-encrusted *G. truncatulinoides* compared to the symbiont-bearing species, *G. ruber* (p) and *O. universa*, which is consistent with a higher microen-
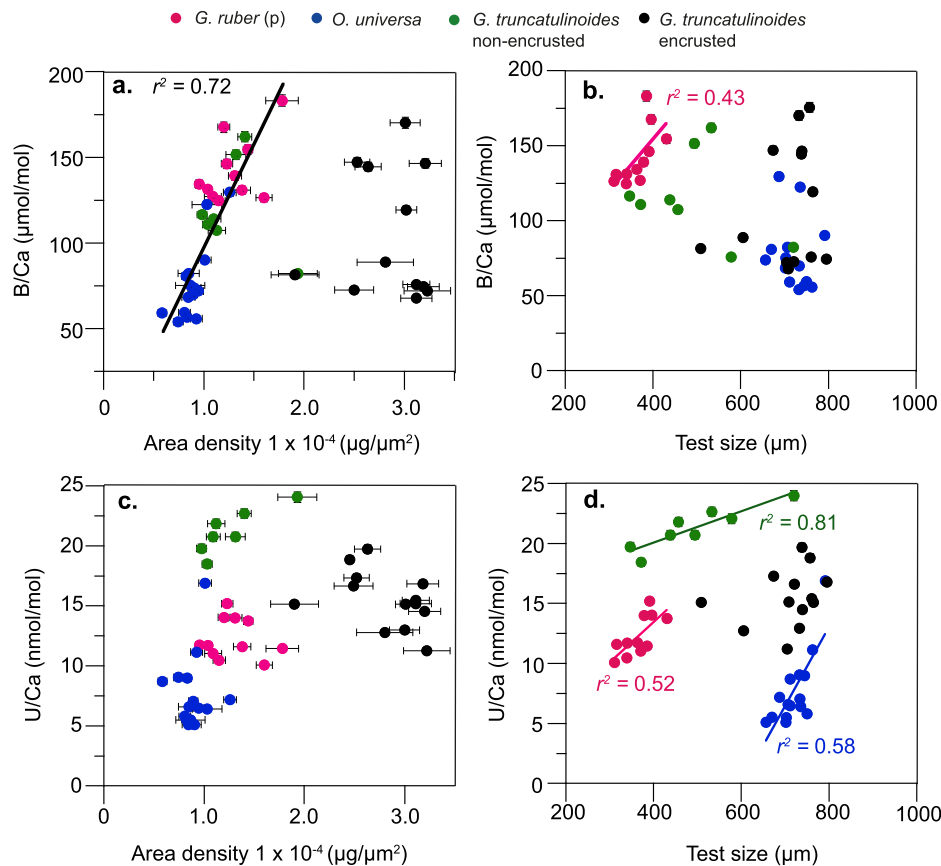
Fig. 4. Linear regressions of **a)** B/Ca and area density of *G. ruber* (p), *O. universa, G. truncatulinoides* non-encrusted. Encrusted *G. truncatulinoides* are shown in black but are not included in the regression. **b)** B/Ca with test size for all species. The only significant regression is in *G. ruber* (p) **c)** U/Ca and area density for all species with only *G. truncatulinoides* non-encrusted/encrusted included in the regression. **d)** Individual species' shell size regressions with U/Ca of *G. ruber* (p), *O. universa, G. truncatulinoides* non-encrusted/encrusted. Errors on area density measurements are AD $\pm (1/n)$, and B/Ca $= \pm 1.84\%$, U/Ca $= 1.79\%$ ($\pm \sigma$).

vironment pH in symbiont-bearing species (Fig. 4d). However, if U/Ca were predominantly controlled by the microenvironment pH, we would expect U/Ca to decrease with increasing test size, due to a higher pH in larger tests of symbiont-bearing species (Henehan et al., 2013). Yet our observations indicate the reverse, displaying a strong species-specific increase in U/Ca with larger test sizes in all species (excluding encrusted *G. truncatulinoides*) but for B/Ca, only in *G. ruber* (p) (Fig. 4d). Additionally, the symbiont-bearing species tend to experience a proportionally greater increase in U/Ca with larger test size, than non-encrusted *G. truncatulinoides* do (Fig. 4d). This indicates a stronger species-specific growth control on U compared to B incorporation. A calcification control is unlikely to explain U/Ca variability in symbiont-bearing species because it does not share a significant relationship with area density (Table 1 − *O. universa* only, Fig. 4c). Furthermore, unlike B/Ca, U/Ca is inversely related to $[CO_3^{2-}]$ (Russell et al., 2004); because tests calcify thicker shells (potentially at faster rates) in higher $[CO_3^{2-}]$ conditions (Marshall et al., 2013), it would be counter-intuitive for an increase in U/Ca to be attributed to faster calcification rates as suggested by Ni et al. (2007). Our results suggest that the incorporation of B is distinctly different from U, because the size-dependent, species-specific relationships are more apparent in foraminiferal U/Ca, compared to B/Ca (Fig. 4d). Based on larger shells representing faster growth (Schmidt et al., 2008), rate-dependent discrimination can act against the biological pumping of larger ions by the cell (Rickaby et al., 2002; Ni et al., 2007), which may explain greater U incorporation in larger foraminifera tests. However, it is still unclear why this mechanism would selectively favour U over B incorporation in larger tests. Future studies should therefore concentrate on determining which cellular pro-

cesses contribute to variations in foraminifera test size and area density and how these relate to different incorporation strategies for B and U.

Overall, our results suggest more research is needed to quantify the impacts of calcification and biological fractionation on the incorporation of B and U before they can be used effectively as carbonate system proxies.

4.2.2. Crust and size control in G. truncatulinoides

Mature individuals of *G. truncatulinoides* form a secondary crust as they descend deeper in the water column, the composition of which can be chemically distinct from the primary calcite for some trace elements (Spear et al., 2011). Yet, we find similar range of B/Ca in both non-encrusted and encrusted *G. truncatulinoides*, whilst U is depleted in encrusted individuals (Fig. 4a, c). If U incorporation was controlled by $[CO_3^{2-}]$, we would expect encrusted individuals to contain higher U/Ca but this is not the case. Our results indicate that the addition of secondary crust does not significantly affect the bulk test B/Ca, but does affect U concentration, further supporting different controls on B and U incorporation. For instance, the B/Ca of encrusted individuals could conceivably reflect the original area density from the non-encrusted stage, with the addition of the secondary crust tripling the area density without increasing the boron concentration (Fig. 4a). Unlike their non-encrusted equivalents, encrusted *G. truncatulinoides* have a large range of B/Ca; the 100 μmol/mol range of B/Ca in encrusted individuals almost encompasses the entire 110 μmol/mol range of B/Ca in non-encrusted, *O. universa* and *G. ruber* (pink) combined (Fig. 4a). Other encrusted globorotaliid species, such as *G. inflata* and *G. scitula* have also shown large intratest B/Ca

variability (Hathorne et al., 2009; Allen et al., 2011), even when grown under identical conditions (Allen et al., 2011), suggesting this heterogeneity could reflect biological changes in the micro-environment, rather than an external environmental control. The depletion in U in encrusted *G. truncatulinoides* could be explained by dilution of [U] when the secondary crust is added. Further research using laser ablation is needed to determine if there are lower concentrations of U in the secondary, compared to the primary calcite.

5. Conclusions

Here we aimed to resolve conflicting interpretations of the controls on B/Ca and U/Ca in three species of planktonic foraminifera *G. ruber* (p), *O. universa*, *G. truncatulinoides* (non-encrusted and encrusted), and evaluate their use as proxies for ocean carbonate chemistry.

We find that species-specific B/Ca is not related to in-situ carbonate chemistry variations during the calcification of planktonic foraminifer tests in this study or collectively when other studies (such as those from core-top sediments) are taken into account. Instead, we suggest that boron incorporation is likely to be controlled by calcification rate owing to a strong positive correlation with test area density (thickness). We find little dependence of B/Ca on test size, except in *G. ruber* (pink).

We find significant increases of U/Ca with test size in all species ($r^2 = 0.52$–0.81), indicating some other biological control (perhaps related to growth) on incorporation of U compared to B. Our study is the first to show that both area density (proxy for test thickness) and test size may affect the incorporation of trace elements differently whereas previously, only changes in test size have been thought to affect trace element composition of planktonic foraminifera.

We recommend that future work should utilise planktonic foraminifera from narrow test thickness and size windows in order to isolate the dominant environmental controls on B and U incorporation in planktonic foraminifera. Our findings caution against the use of fossil planktonic foraminifera B/Ca and U/Ca as reliable proxies for the carbonate system until we have an improved mechanistic understanding of how calcification and growth rates regulate boron and uranium incorporation into the foraminifer test.

Acknowledgements

Appendix A. Supplementary material

Supplementary material related to this article can be found online at http://dx.doi.org/10.1016/j.epsl.2016.05.016.

References

Akaike, H., 1974. A new look at the statistical model identification. IEEE Trans. Autom. Control 19 (6), 716–723. http://dx.doi.org/10.1109/TAC.1974.1100705.

Allen, K.A., Hönisch, B., Eggins, S.M., Yu, J., Spero, H.J., Elderfield, H., 2011. Controls on boron incorporation in cultured tests of the planktic foraminifer *Orbulina universa*. Earth Planet. Sci. Lett. 309, 291–301.

Allen, K.A., Hönisch, B., 2012. The planktic foraminiferal B/Ca proxy for seawater carbonate chemistry: a critical evaluation. Earth Planet. Sci. Lett. 345–348, 203–211.

Allen, K.A., Hönisch, B., Eggins, S.M., Rosenthal, Y., 2012. Environmental controls on B/Ca in calcite tests of the tropical planktic foraminifer species *Globigerinoides ruber* and *Globigerinoides sacculifer*. Earth Planet. Sci. Lett. 351–352, 270–280.

Anand, P., Elderfield, H., Conte, M.H., 2003. Calibration of Mg/Ca thermometry in planktonic foraminifera from a sediment trap time series. Paleoceanography 18, 1050. http://dx.doi.org/10.1029/2002PA000846.

Arbuszewski, J., deMenocal, P., Kaplan, A., Farmer, E.C., 2010. On the fidelity of shell-derived $\delta^{18}O_{seawater}$ estimates. Earth Planet. Sci. Lett. 300, 185–196.

Babila, T.L., Rosenthal, Y., Conte, M.H., 2014. Evaluation of the biogeochemical controls on B/Ca of *Globigerinoides ruber* white from the Oceanic Flux Program, Bermuda. Earth Planet. Sci. Lett. 404, 67–76.

Barker, S., Elderfield, H., 2002. Foraminiferal calcification response to Glacial–Interglacial ranges in atmospheric CO_2. Science 297, 833–836.

Barker, S., Greaves, M., Elderfield, H., 2003. A study of cleaning procedures used for foraminiferal Mg/Ca paleothermometry. Geochem. Geophys. Geosyst. 4, 1525–2027.

Beer, C.J., Schiebel, R., Wilson, P.A., 2010. Technical note: on methodologies for determining size-normalised weight of planktic foraminifera. Biogeosciences 7, 2193–2198.

Bemis, B.E., Spero, H.J., Bijma, J., Lea, D.W., 1998. Reevaluation of the oxygen isotopic composition of planktonic foraminifera: experimental results and revised paleotemperature equations. Paleoceanography 13, 150–160.

Branson, O., Kaczmarek, K., Redfern, S.A.T., Misra, S., Langer, G., Tyliszczak, T., Bijma, J., Elderfield, H., 2015. The coordination and distribution of B in foraminiferal calcite. Earth Planet. Sci. Lett. 416, 67–72.

Dickson, A.G., Millero, F.J., 1987. A comparison of the equilibrium constants for the dissociation of the carbonic acid in seawater media. Deep-Sea Res., A, Oceanogr. Res. Pap. 34, 1733–1743.

Dickson, A.G., 1990. Thermodynamics of the dissociation of boric acid in synthetic seawater from 273.15 K to 318.15 K. Deep-Sea Res., Part A 37, 755–766.

Elderfield, H., Vautravers, M., Cooper, M., 2002. The relationship between shell size and Mg/Ca, Sr/Ca, D18O, and D13C of species of planktonic foraminifera. Geochem. Geophys. Geosyst. 3, 1525–2027. http://dx.doi.org/10.1029/2001GC000194.

Foster, G.L., 2008. Seawater pH, pCO_2 and $[CO_3^{2-}]$ variations in the Caribbean Sea over the last 130 kyr: a boron isotope and B/Ca study of planktic foraminifera. Earth Planet. Sci. Lett. 271, 254–266.

Friedrich, O., Schiebel, R., Wilson, P.A., Weldeab, S., Beer, C.J., Cooper, M.J., Fiebig, J., 2012. Influence of test size, water depth, and ecology on Mg/Ca, Sr/Ca, $\delta^{18}O$ and $\delta^{13}C$ in nine modern species of planktic foraminifers. Earth Planet. Sci. Lett. 319–320, 133–145.

Gabitov, R.I., Rollion-Bard, C., Tripati, A., Sadekov, A., 2014. In situ study of boron partitioning between calcite and fluid at different crystal growth rates. Geochim. Cosmochim. Acta 137, 81–92.

Hathorne, E.C., James, R.H., Lampitt, R.S., 2009. Environmental versus biomineralization controls on the intratest variation in the trace element composition of the planktonic foraminifera *G. inflata* and *G. scitula*. Paleoceanography 24, PA4202. http://dx.doi.org/10.1029/2009PA001742.

Hemleben, C., Spindler, M., Breitinger, I., W.G., 1985. Field and laboratory studies on the ontogeny and ecology of some Globorotaliid species from the Sargasso Sea off Bermuda. J. Foraminiferal Res. 15, 254–272.

Hemming, N.G., Hanson, G.N., 1992. Boron isotopic composition and concentration in modern marine carbonates. Geochim. Cosmochim. Acta 56 (1), 537–543. http://dx.doi.org/10.1016/0016-7037(92)90151-8.

Henehan, M.J., Rae, J.W.B., Foster, G.L., Erez, J., Prentice, K.C., Kucera, M., Bostoc, H.C., Martínez-Botí, M.A., Milton, J.A., Wilson, P.A., Marhsall, B.J., Elliott, T., 2013. Calibration of the boron isotope proxy in the planktonic foraminifera *Globigerinoides ruber* for use in palaeo-CO_2 reconstruction. Earth Planet. Sci. Lett. 364, 111–122.

Henehan, M.J., Foster, G.L., Rae, J.W.B., Prentice, K.C., Erez, J., Bostock, H.C., Marshall, B.J., Wilson, P.A., 2015. Evaluating the utility of B/Ca ratios in planktic foraminifera as a proxy for the carbonate system: a case study of *Globigerinoides ruber*. Geochem. Geophys. Geosyst. 16. http://dx.doi.org/10.1002/2014GC005514.

Jonkers, L., Kučera, M., 2015. Global analysis of seasonality in the shell flux of extant planktonic Foraminifera. Biogeosciences 12, 2207–2226.

King, A., Howard, W., 2005. $\delta^{18}O$ seasonality of planktonic foraminifera from Southern Ocean sediment traps: latitudinal gradients and implications for paleoclimate reconstructions. Mar. Micropaleontol. 56, 1–24.

Marshall, B.J., Thunell, R.C., Henehan, M.J., Astor, Y., Wejnert, K.E., 2013. Planktonic foraminiferal area density as a proxy for carbonate ion concentration: a cali-

bration study using the Cariaco Basin ocean time series. Paleoceanography 28, 1–14.

McKenna, V.S., Prell, W.L., 2004. Calibration of the Mg/Ca of *Globorotalia truncatulinoides* (R) for the reconstruction of marine temperature gradients. Paleoceanography 19. http://dx.doi.org/10.1029/2000PA000604.

Mehrbach, C., Culberson, C.H., Hawley, J.E., Pytkowicz, R.M., 1973. Measurement of the apparent dissociation constants of carbonic acid seawater at atmospheric pressure. Limnol. Oceanogr. 18, 897–907.

Misra, S., Greaves, M., Owen, R., Kerr, J., Elmore, A.C., Elderfield, H., 2014. Determination of B/Ca of natural carbonates by HR-ICP-MS. Geochem. Geophys. Geosyst. 15, 1617–1628.

Morard, R., Quillévéré, F., Escarguel, G., Ujiie, Y., de Garidel-Thoren, T., Norris, R.D., de Vargas, C., 2009. Morphological recognition of cryptic species in the planktonic foraminifer *Orbulina universa*. Mar. Micropaleontol. 71, 148–165.

Naik, S.S., Naidu, P.D., 2014. Boron/calcium ratios in *Globigerinoides ruber* from the Arabian Sea: implications for controls on boron incorporation. Mar. Micropaleontol. 107, 1–7.

Ni, Y., Foster, G.L., Bailey, T., Elliott, T., Schmidt, D.N., Pearson, P., Haley, B., Coath, C., 2007. A core top assessment of proxies for the ocean carbonate system in surface-dwelling foraminifers. Paleoceanography 22, PA3212. http://dx.doi.org/10.1029/2006PA001337.

O'Neil, J.R., Clayton, R.N., Mayeda, T.K., 1969. Oxygen isotope fractionation in divalent metal carbonates. J. Chem. Phys. 51, 5547–5558.

Pelletier, G., Lewis, E., Wallace, D., 2007. CO2sys_ver16.xls: a calculator for the CO_2 system in seawater for Microsoft Excel/VBA. Washington State Department of Ecology/Brookhaven National Laboratory, Olympia, WA/Upton, NY, USA.

Rae, J.W.B., Foster, G.L., Schmidt, D.N., Elliott, T., 2011. Boron isotopes and B/Ca in benthic foraminifera: proxies for the deep ocean carbonate system. Earth Planet. Sci. Lett. 302, 403–413.

Rickaby, R.E.M., Schrag, D.P., Zondervan, I., Riebesell, U., 2002. Growth rate dependence of Sr incorporation during calcification of *Emiliania huxleyi*. 16, 1006. http://dx.doi.org/10.1029/2001GB001408.

Ruiz-Agudo, E., Putnis, C.V., Kowacz, M., Ortega-Huertas, M., Putnis, A., 2012. Boron incorporation into calcite during growth: implications for the use of boron in carbonates as a pH proxy. Earth Planet. Sci. Lett. 345–348, 9–17.

Russell, A.D., Emerson, S., Mix, A.C., Peterson, L.C., 1996. The use of foraminiferal U/Ca as an indicator of changes in seawater U content. Paleoceanography 11, 649–663.

Russell, A.D., Hönisch, B., Spero, H.J., Lea, D.W., 2004. Effects of seawater carbonate ion concentration and temperature on shell U, Mg, and Sr in cultured planktonic foraminifera. Geochim. Cosmochim. Acta 68, 4347–4361.

Salmon, K.H., Anand, P., Sexton, P.F., Conte, M., 2015. Upper ocean mixing controls the seasonality of planktonic foraminifer fluxes and associated strength of the carbonate pump in the oligotrophic North Atlantic. Biogeosciences 12, 1–13.

Sanyal, A., Hemming, N.G., Broecker, W.S., Hanson, G.N., 1997. Changes in pH in the eastern equatorial Pacific across stage 5–6 boundary based on boron isotopes in foraminifera. Glob. Biogeochem. Cycles 11, 125–133.

Sanyal, A., Nugent, M., Reeder, R., Bijma, J., 2000. Seawater pH control on the boron isotopic composition of calcite: evidence from inorganic calcite precipitation experiments. Geochim. Cosmochim. Acta 64 (9), 1551–1555. http://dx.doi.org/10.1016/S0016-7037(99)00437-8.

Schmidt, G.A., Bigg, G.R., Rohling, E.J., 1999. Global seawater oxygen-18 database – v1.21.

Schmidt, D.N., Elliott, T., Kasemann, S.A., 2008. The influences of growth rates on planktic foraminifers as proxies for palaeostudies – a review. Geol. Soc. (Lond.) Spec. Publ. 303, 73–85. http://dx.doi.org/10.1144/SP303.6.

Shackleton, N.J., 1974. Attainment of isotopic equilibrium between ocean water and the benthonic foraminiferal genus Uvigerina: isotopic changes in the ocean during the last glacial. In: Colloque international du CNRS, vol. 219, pp. 203–210.

Spear, J.W., Poore, R.Z., Quinn, T.M., 2011. *Globorotalia truncatulinoides* (dextral) Mg/Ca as a proxy for Gulf of Mexico winter mixed-layer temperature: evidence from a sediment trap in the northern Gulf of Mexico. Mar. Micropaleontol. 80, 53–61.

Spero, H.J., Parker, S.L., 1985. Photosynthesis in the symbiotic planktonic foraminifer *Orbulina universa*, and its potential contribution to oceanic primary productivity. J. Foraminiferal Res. 15, 273–281.

Spero, H.J., Bijma, J., Lea, D.W., Bemis, B.E., 1997. Effect of seawater carbonate concentration on foraminiferal carbon and oxygen isotopes. Nature 390, 497–500.

Steinberg, D.K., Carlson, C.A., Bates, N.R., Rodney, J.J., Michaels, A.F., Knap, A.H., 2001. Overview of the US JGOFS Bermuda Atlantic Time-series Study (BATS): a decade-scale look at ocean biology and biogeochemistry. Deep-Sea Res., II 48, 1405–1447.

Takahashi, K., Bé, A.W.H., 1984. Planktonic foraminifera: factors controlling sinking speeds. Deep-Sea Res. 31, 1477–1500.

Ujiié, Y., de Garidel-Thoron, T., Watanabe, S., Wiebe, P., de Vargas, C., 2010. Coiling dimorphism within a genetic type of the planktonic foraminifer *Globorotalia truncatulinoides*. Mar. Micropaleontol. 77, 145–153.

Yu, J., Elderfield, H., Hönisch, B., 2007. B/Ca in planktonic foraminifera as a proxy for surface seawater pH. Paleoceanography 22, PA2202. http://dx.doi.org/10.1029/2006PA001347.

Yu, J., Elderfield, H., Jin, Z., Booth, L., 2008. A strong temperature effect on U/Ca in planktonic foraminiferal carbonates. Geochim. Cosmochim. Acta 72, 4988–5000.

Yu, J., Thornalley, D.J.R., Rae, J.W.B., McCave, N.I., 2013. Calibration and application of B/Ca, Cd/Ca, and δ^{11}B in *Neogloboquadrina pachyderma* (sinistral) to constrain CO_2 uptake in the subpolar North Atlantic during the last deglaciation. Paleoceanography 28, 1–16. http://dx.doi.org/10.1002/palo.20024.

Further reading

Bacastow, R.B., Keeling, C.D., Lueker, T.J., Wahlen, M., Mook, W.G., 1996. The ^{13}C Suess effect in the world surface oceans and its implications for oceanic uptake of CO_2: analysis of observations at Bermuda. Glob. Biogeochem. Cycles 10, 335–346.